Transmission electron energy-loss spectroscopy study of carbon nanotubes upon high temperature treatment

B. W. Reed, M. Sarikaya, L. R. Dalton, and G. F. Bertsch

Citation: Appl. Phys. Lett. **78**, 3358 (2001); doi: 10.1063/1.1372618
View online: https://doi.org/10.1063/1.1372618
View Table of Contents: http://aip.scitation.org/toc/apl/78/21
Published by the American Institute of Physics

Transmission electron energy-loss spectroscopy study of carbon nanotubes upon high temperature treatment

B. W. Reed, M. Sarikaya,[a] L. R. Dalton,[b] and G. F. Bertsch[c]
Materials Science and Engineering, University of Washington, Seattle, Washington 98195

(Received 25 September 2000; accepted for publication 26 March 2001)

Two batches of carbon nanotube materials, grown with a pulsed-laser deposition technique but purified and heat treated under different conditions, are investigated with a combination of high-resolution transmission electron microscopy techniques, including electron nanodiffraction and low-loss and carbon *K*-edge electron energy-loss spectroscopy. These techniques were used to achieve a detailed profile of each material. Heat treating one batch at 1100 °C is shown to increase the sp^2/sp^3 hybridization ratio, while a 2150 °C treatment of the other batch fundamentally restructured the material from single walled to a mixture of amorphous and multiwalled material. © *2001 American Institute of Physics.* [DOI: 10.1063/1.1372618]

Since their discovery,[1] carbon nanotubes have attracted much attention. Many studies have been undertaken in order to optimize growth conditions,[2–4] elucidate physical structure, and measure electronic properties.[5–10] Most investigations have been quite specific, centering on a small number of nanotubes formed under particular conditions and typically employing only one or two modes of analysis. Broader, more systematic studies are relatively rare, and it is the intent of the present work to help fill this gap. We combine results of high-resolution transmission electron microscopy (TEM) imaging, low-energy electron energy-loss spectroscopy (EELS), carbon *K*-edge EELS, and electron nanodiffraction to characterize a variety of nanotube samples, purified and heat treated under various conditions. Our intent was to develop a complete profile of each material. Comparing profiles from differently prepared materials reveals patterns that might be overlooked in a more tightly focused, less systematic effort. In particular, we show that the heat treatment step has significant effects on both the structural and the electronic properties of the material.

Two batches (A and B) of carbon nanotubes were differently purified and high-temperature treated. Both carbon nanotube samples were made by the dual pulsed-laser vaporization method, which provides a high yield (20%) of single-walled carbon nanotubes.[11,12] Both batches were purified with a process that involves nitric acid reflux followed by washing/centrifugation cycles increasing yield to 60%. Batch B was further purified using a hollow-fiber cross-flow filtration technique that yields 1 μm thick high-purity single-walled nanotube papers.[11–13] Because of their piezoelectric characteristics, a promising application of these nanotube papers is high-temperature actuators.[14] A high-temperature baking procedure (1100 °C, Ar atmosphere, 1 h) is usually carried out to eliminate oxidatively intercalated acid molecules and impurity fullerenes (e.g., C_{60}) while the metal catalyst particles are eliminated during the acid reflux cycle. Batch A is also heat treated at 2150 °C (in Ar, 1 h) in an attempt to eliminate impurities, allowing us to compare the effects of filtration and high-temperature treatment. High-temperature treatments also affect structural stability and temperature-dependent physical properties such as electrical conductivity.[12] Rather than the bulk characterization usually carried out in the literature, our work focused to assess local structures and properties of individual tubes or their clusters upon high-temperature treatment using the high-resolution methods described below.

The measurements were performed in a Topcon 002B TEM fitted with a Gatan Image Filter for parallel EELS. The sample was illuminated with an electron probe of diameter 3.3 nm [full width at half maximum (FWHM)] at 200 kV. The intermediate lenses were operating in diffraction mode, while the smallest spectrometer aperture, 0.6 mm, was used. Under these conditions, the energy resolution of the spectrometer was 1.0 eV (FWHM of the zero-loss peak) or more, depending on the gun current. The incident and collection semiangles were 8.6 and 2.0 mrad, respectively. Using a small probe (a few nanometer-diameter) electron nanodiffraction patterns were obtained from nanotube clusters, to characterize the nanotube structure and stability under the electron beam.

Since our aim was to show differences in nanotube materials formed under different conditions, we had to ensure that any apparent pattern was characteristic of our material, rather than an apparent difference due to peculiar structures or orientations at the points chosen for analysis. We chose multiple points for EELS measurements on each sample, with widely varying local geometry.

The *K*-edge spectra were sharpened by Fourier-ratio deconvolution[15] with the low-loss spectra using the standard routines in the commercial software package EL/P.[16] The zero-loss background was subtracted from the low-loss spectra using a variation on a spline curve fit technique reported previously.[17] The details of the current procedure will be presented elsewhere.

Typical TEM images of the nanotube samples are shown in Figs. 1(a)–1(d). All but one are made almost entirely of single-walled nanotubes, mostly arranged in parallel bundles. The 1100 °C treatment performed on half of batch B had no

[a]Electronic mail: sarikaya@u.washington.edu
[b]Department of Chemistry, University of Washington, Seattle, WA 98195.
[c]Department of Physics, University of Washington, Seattle, WA 98195.

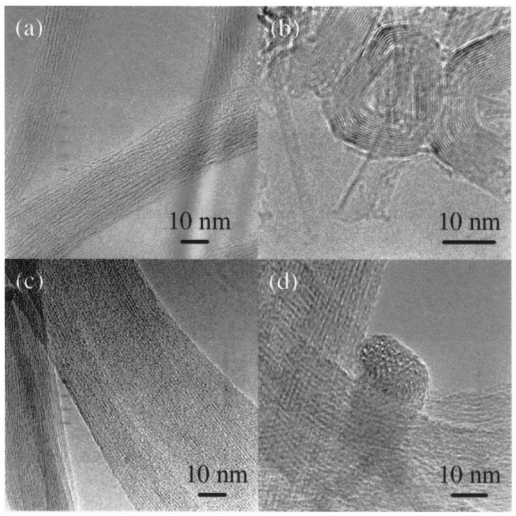

FIG. 1. TEM images of carbon nanotube material with various purification and heat treatment conditions. (a) Batch A, 1100 °C heat treatment. (b) Batch A, 2150 °C treatment. (c) Batch B, as received. (d) Batch B, 1100 °C treatment.

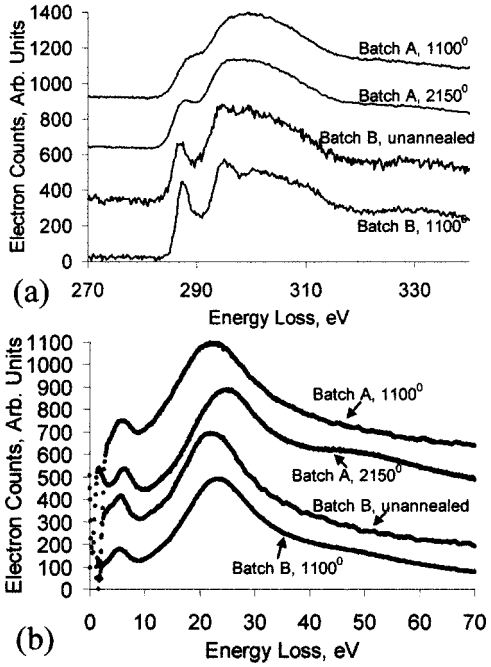

FIG. 2. (a) Carbon *K*-edge near-edge EELS profiles and (b) low-loss EELS for the four samples. The *Y* axis is offset for each profile.

apparent effect on the physical structure as seen in phase-contrast TEM images. The low-temperature-treated batch A sample looks much like the samples from batch B, although perhaps with more surface contamination and less uniformity. The 2150 °C treatment on batch A appears to have entirely rearranged the material into a mixture of amorphous carbon, irregular multiwalled ''bucky onion'' structures, some very wide but short single-wall tubes, and a few multiwalled tubes of poor uniformity. This sample showed vastly more variety of structure than did any of the others. Similar rearrangements have been reported by other groups.[18,19]

The carbon *K*-edge spectra reveal differences that do not appear in the images, as shown in Fig. 2(a). Differences in signal-to-noise ratio are due to differences in mass thickness, as all the spectra were acquired for the same duration (10 s) with similar beam current. The line shapes are found to be independent of mass thickness in the limit of single scattering. The most obvious (and repeatable) difference among the profiles is the strength of the initial peak, which is due to $1s \rightarrow 2\pi^*$ transitions, and is a good measure of the fraction of sp^2 hybridization in the material.[20,21] Since an ideal nanotube is purely sp^2 hybridized, this peak should be strong for a highly crystalline material and weaker for a material with impurities, dangling bonds, and other defects. The strongest π^* peak occurs in the 1100 °C-treated batch B sample and the second strongest in the untreated batch B, with both batch A samples showing weak π^* responses. The 1100 °C heat treatment appears to have healed many of the defects in batch B (eliminating remains of acid flux treatment and impurity fullerenes), bringing the material closer to the ideal of pure sp^2 hybridization, without an apparent change in nanoscale morphology as seen in the phase-contrast images. The bonding in batch A appears to be much like that in amorphous carbon, with the high-temperature treatment producing a modest increase in the sp^2 hybridization.

Additional information about the electronic structure can be found in the low-loss EELS. These measurements show two distinct plasmon responses, with the π electrons responding at ~5–6 eV and the π and σ at ~24 eV. The energies of the plasmon modes are related to the densities of the involved electrons, but are also modified by the extreme surface curvature and surface-to-bulk ratio of a nanotube.[6,7] A high-quality single-walled nanotube material (the heat-treated batch B) should show a strong π plasmon, but at a slightly lower energy than the corresponding plasmon in graphite and similar materials. Multiwalled material (the high-temperature-treated batch A) should behave more like graphite, with plasmon energies closer to graphite's 6.5 and 26 eV. The measurements summarized in Table I confirm this. The $\pi+\sigma$ plasmon energy, a measure of total valence electron density, increases with increased treatment temperature. The relative strength of the π plasmon also appears to increase with increased treatment temperature, though the trend is weak.

Finally, we performed nanodiffraction on our samples, focusing an electron probe of diameter varying from 3 to 10 nm onto individual nanotube bundles [Fig. 3(a)]. Other than the obvious geometry effect of the cylindrical bundle, there is little departure from circular symmetry, even in the heat-treated batch B sample. This result was independent of electron dose—this type of pattern appears the first instant that the probe touches any particular bundle. A selected-area diffraction pattern of a large straight bundle [Fig. 3(b)] shows well-defined spots with no strongly preferred orientation, and

TABLE I. Energies and peak height ratios for the plasmons in the four materials investigated. Uncertainties are sample standard deviations of the means.

Batch	Heat treatment (°C)	π plasmon energy (eV)	$\pi+\sigma$ plasmon energy (eV)	$\pi/(\pi+\sigma)$ peak height ratio
A	1100	5.7±0.2	22.5±0.3	0.3±0.1
A	2150	6.2±0.2	24.3±0.3	0.4±0.1
B	none	5.7±0.2	22.0±0.2	0.35±0.1
B	1100	5.2±0.2	23.1±0.2	0.4±0.1

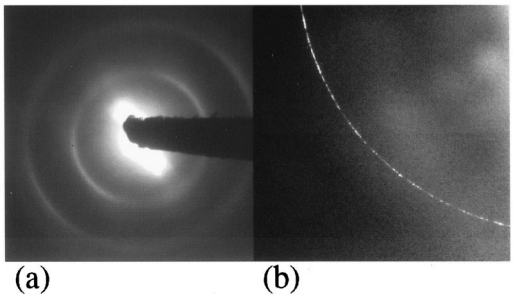

FIG. 3. (a) Nanodiffraction and (b) closeup of part of a selected area diffraction pattern from bundles of parallel tubes in the 1100 °C-treated batch B sample.

this also is independent of dose for the radiation densities and durations we used. What this suggests is that the chiral angles within the bundles are highly random, in contrast to what other researchers have seen in their nanotube material,[18] and that the material is adequately stable under the electron beam.

Combining these modes of characterization, then, we can form a profile of each material and make comparisons. The 1100 °C-treated batch B sample is the best approximation to the ideal pure single-walled nanotube material, with a high fraction of sp^2 hybridization, a plasmon structure consistent with highly curved graphene sheets, and very uniform-looking bundles of tubes, although the distribution of chiral angles within the bundles appears to be random. The untreated batch B, while physically similar, apparently has some defects (possibly surface impurities) that are revealed as reduced π character in the EEL spectra. The 1100 °C-treated batch A, while looking much like the batch B samples, is a lower-quality material all around, with very weak π response in both the plasmons and the carbon *K* edge, possibly due to impurity materials which are not usually seen in low-resolution TEM images without the additional EELS analysis. The high-temperature-treated batch A has restructured itself into a mixture of amorphous carbon and multiwalled structures, and gives an EELS profile consistent with graphite-like amorphous carbon. Increased treatment temperature increased the π character of both batches.

By combining high-resolution imaging with nanodiffraction and low-loss and carbon *K*-edge EELS, we have locally characterized a number of nanotube materials formed and heat treated under various conditions. The effects of the high-temperature treatment are visible in both the physical structure and the electronic properties. The more characterization techniques used and the more samples with differing preparation histories considered, the clearer are the trends one can see in the structures and properties of the nanotube materials—patterns that might not be apparent in a traditional, more tightly focused bulk spectroscopic study. Our aim at this time is more to characterize the material that results from various fabrication techniques than to explore the fundamental physics of the nanotubes, the latter being our future focus. The information presented herein should be of value in understanding how the tubes form and in optimizing the conditions for producing high-quality material for closer investigation of structure–property relations and for potential real-life applications.

This work was supported by NSF Grant No. DMR 9978835.

[1] S. Iijima, Nature (London) **354**, 56 (1991).
[2] R. Saito, G. Dresselhaus, and M. S. Dresselhaus, *Physical Properties of Carbon Nanotubes* (Imperial College, London, 1998).
[3] P. G. Collins, J. C. Grossman, M. Cote, M. Ishigami, C. Piskoti, S. G. Louie, M. L. Cohen, and A. Zettl, Phys. Rev. Lett. **82**, 165 (1999).
[4] H. Yoshioka and A. A. Odinstov, Phys. Rev. Lett. **82**, 374 (1999).
[5] R. Kuzuo, M. Terauchi, and M. Tanaka, Jpn. J. Appl. Phys., Part 2 **31**, L1484 (1992).
[6] P. M. Ajayan, S. Iijima, and T. Ichihashi, Phys. Rev. B **47**, 6859 (1993).
[7] L. A. Bursill, P. A. Stadelmann, J. L. Peng, and S. Prawer, Phys. Rev. B **49**, 2882 (1994).
[8] T. Pichler, M. Knupfer, M. S. Golden, J. Fink, A. Rinzler, and R. E. Smalley, Phys. Rev. Lett. **80**, 4729 (1998).
[9] K. Yase, S. Horiuchi, M. Kyotani, M. Yumura, K. Uchida, S. Ohshima, Y. Kuriki, F. Ikazaki, and N. Yamahira, Thin Solid Films **273**, 222 (1996).
[10] M. Kociak, L. Henrard, O. Stephan, K. Suenaga, and C. Colliex, Phys. Rev. B **61**, 13 936 (2000).
[11] J. Liu, A. G. Rinzler, H. Dai, J. H. Hafner, R. K. Bradley, P. J. Boul, A. Lu, T. Iverson, K. Shelimov, C. B. Huffman, F. Rodriguez-Macias, Y.-S. Shon, T. R. Lee, D. T. Colbert, and R. E. Smalley, Science **280**, 1253 (1999).
[12] A. G. Rinzler, J. Liu, H. Dai, C. B. Huffman, F. J. Rodriguez-Macias, P. J. Boul, A. H. Lu, D. Heymann, D. T. Colbert, R. S. Lee, J. E. Fischer, A. M. Rao, P. C. Eklund, and R. E. Smalley, Appl. Phys. A: Mater. Sci. Process. **67**, 29 (1998).
[13] R. H. Baughman, C. Cui, A. A. Zakhidov, Z. Iqbal, J. N. Barisci, G. M. Spinks, G. G. Wallace, A. Mazzoldi, D. De Rossi, A. G. Rinzler, O. Jaschinski, S. Roth, and M. Kertesz, Science **284**, 1340 (1999).
[14] L. Fifield, L. R. Dalton, R. H. Baughman, A. Lobovsky, and G. M. Spinks, Proc. SPIE **3987** (in press).
[15] R. F. Egerton, *Electron Energy Loss Spectroscopy in the Electron Microscope*, Second Edition (Plenum Press, New York, 1996).
[16] EL/P Software (Gatan Inc., Pleasanton, CA, www.gatan.com).
[17] B. W. Reed, J. M. Chen, N. C. MacDonald, J. Silcox, and G. F. Bertsch, Phys. Rev. B **60**, 5641 (1999).
[18] P. Nikolaev, A. Thess, A. G. Rinzler, D. T. Colbert, and R. E. Smalley, Chem. Phys. Lett. **266**, 422 (1997).
[19] M. Zhang, D. W. He, L. Ji, B. Q. Wei, D. H. Wu, X. Y. Zhang, Y. F. Xu, and W. K. Wang, Carbon **37**, 657 (1999).
[20] S. Zhang, X. T. Zeng, H. Xie, and P. Hing, Surf. Coat. Technol. **123**, 256 (2000).
[21] V. Serin, E. Beche, R. Berjoan, O. Abidate, D. Dorignac, D. Rats, J. Fontaine, L. Vandenbulcke, C. Germain, and A. Catherinot, Electrochem. Soc. Proc. **97**, 126 (1998).